PERGAMON

International Journal of Heat and Mass Transfer 43 (2000) 3567–3578

International Journal of HEAT and MASS TRANSFER

www.elsevier.com/locate/ijhmt

Fouling in enhanced tubes using cooling tower water Part I: long-term fouling data

Ralph L. Webb[a,*], Wei Li[b]

[a]Department of Mechanical Engineering, The Pennsylvania State University, University Park, PA 16802, USA
[b]Engineered Air, 320580 W. 83rd St., DeSoto, KS, USA

Received 5 February 1999; received in revised form 10 December 1999

Abstract

This paper describes the results of long-term fouling tests for cooling tower water flowing inside enhanced tubes. The data were taken using 800 ppm calcium hardness water supplied to an operating chiller/cooling tower system. The fouling mechanism is a combination of precipitation fouling and particulate fouling. Fouling data were measured for seven different enhanced tube geometries over a 2500 h operating period. The tubes tested had internal helical ridges, and the number of ridge starts varied from 10 to 45. Little fouling occurred until 1300 h. After 1300 h, moderate fouling began to occur in the tubes having a large number of starts. These tubes also provide the highest water-side heat transfer coefficients. Significant fouling existed in the tubes having 30–45 starts at the end of the test period. The salient finding of this work is that the potential for fouling increases as the number of starts and helix angle increases.

1. Introduction

Use of tube side enhancement is becoming common in water chiller condensers and evaporators. Fig. 1 shows seven internally finned tube geometries that span the range of geometries of present commercial interest. Such tubes are typically used with cooling tower water. Because fouling is a slow process, most fouling studies have been done for accelerated fouling using a very high foulant concentration. This allows significant fouling to occur within several hours or several days. Several investigators have performed accelerated particulate fouling in enhanced tubes, such as Kim and Webb [1], Somerscales [2] and Chamra and Webb [3]. Watkinson [4] performed accelerated precipitation fouling tests on internally enhanced tubes. Morse and Knudsen [5] performed a series of fouling tests with simulated cooling tower water on the exterior of a smooth tube in an annulus. Chapter 10 of Webb [6] summarizes much of the relevant prior work on fouling in enhanced tubes. The accelerated fouling data on enhanced tubes typically show that they foul faster than plain tubes. However, the fouling rate depends on the internal geometry.

The literature is severely lacking in long-term fouling of enhanced tubes using foulant concentrations typical of that in actual operating systems. Rabas et al. [7] made in-plant fouling tests of electric utility steam condenser tubes using river water as foulant. This work compared corrugated and plain tubes. Haider and Webb [8] performed long-term tests of water used in the evaporator tubes of flooded water chillers. This study showed negligible fouling, principally because

* Corresponding author. Tel.: +1-814-865-0283; fax: +1-814-865-1344.
E-mail address: rlwebb@psu.edu (R.L. Webb).

0017-9310/00/$ - see front matter
PII: S0017-9310(99)00395-6

Nomenclature

A	total Inside surface area, m^2
$A_{i,\,nom}$	nominal internal surface area based on plain tube ($=\pi D_i L$), m^2
C_{ST}	Sieder–Tate coefficient used in Eq. (2)
D	tube diameter, m
e	rib height, m
f	friction factor, dimensionless
h	heat transfer coefficient of clean tube based on $A_{i,\,nom}$, W/m^2 K
h_{eff}	effective heat transfer coefficient ($1/h_{eff} = 1/h + R_f$), W/m^2 K
k	thermal conductivity, W/m K
L	tube length, m
n_s	number of starts
p	axial element pitch, m
p_{sat}	saturation or condenser pressure, N/m^2
Pr	Prandtl number, dimensionless
q	heat transfer rate, W
Re	Reynolds number, dimensionless
R_f	fouling resistance based on $A_{i,\,nom}$, m^2 K/W
R_f^*	asymptotic fouling resistance, m^2 K/W
ΔR_i	difference between the $1/U$ values of the two paired tubes at start-up, m^2 K/W
T	temperature, K
ΔT	temperature difference, K
ΔT_{lm}	Log mean temperature difference, K
u	fluid velocity, m/s
U	overall heat transfer coefficient, W/m^2 K

Greek symbols

α	helix angle, degrees
η	efficiency index, $(h/h_p)/(f/f_p)$, dimensionless
μ	dynamic viscosity at bulk water temperature, kg/m s
μ_w	dynamic viscosity at wall temperature, kg/m s
θ_D	fouling induction period, h
σ	standard deviation unit

Subscripts

b	bulk
c	clean
f	fouled
p	plain surface

the water was very clean and particulate fouling was the only possible fouling mechanism.

The present work addresses long-term fouling of cooling tower water in a refrigerant condenser having enhanced tubes. The tubes tested are shown in Fig. 1. The fouling tests were performed in a separate fouling condenser, using the cooling tower water supplied to the main refrigerant condenser.

2. Fouling test program

The apparatus was located in the Walker Building on the Penn State University campus. Located in that building is a 880 kW (250 ton) R-11 centrifugal Carrier refrigeration unit that cools the building. The fouling test condenser was connected in parallel with the condenser of the water chiller. This condenser, and that in chiller system, contained 3.66 m (12.0 ft) long tubes. The cooling tower water supplied to the main refrigerant condenser was also supplied to the tubes in the fouling condenser. Seven different enhanced tube geometries were contained in the fouling test condenser.

The fouling mechanisms possible in a cooling tower water condenser conceivably may be precipitation fouling, biological fouling, corrosion fouling, and particulate fouling. In a practical sense, only two mechanisms were expected in the present tests — precipitation and particulate fouling. This is because the water was treated with corrosion inhibitors and biocides. These acted to inhibit corrosion and biological fouling. Precipitation fouling is expected in cooling tower systems. The heated water will precipitate $CaCO_3$ or $MgCO_3$ salts contained in the water. Particulate fouling is also expected, because of airborne dust exposed to the water in the cooling tower. Hence, the present interests are primarily limited to the combination of precipitation fouling and particulate fouling.

3. Tube geometries tested

Fig. 1 shows the internally enhanced tube geometries tested in this work. The geometry details are defined in Table 1. The geometries vary the number of starts (n_s), helix angle (α), and fin height (e). Tube 1 has a plain interior surface and the other seven have internal enhancement. All eight tubes have 1023 fins/m (26 fins/in.), 0.9 mm high on the outer surface. The geometry dimensions of the tubes are summarized in Table 1. As the number of fin starts increase, the fins are more closely spaced, and the internal surface area increases.

These tubes provide water-side enhancement in the range of 70–130%. Tube 4 having 10 thread starts is typical of the geometry used in the early 1980s. Advances in manufacture have resulted in tubes having

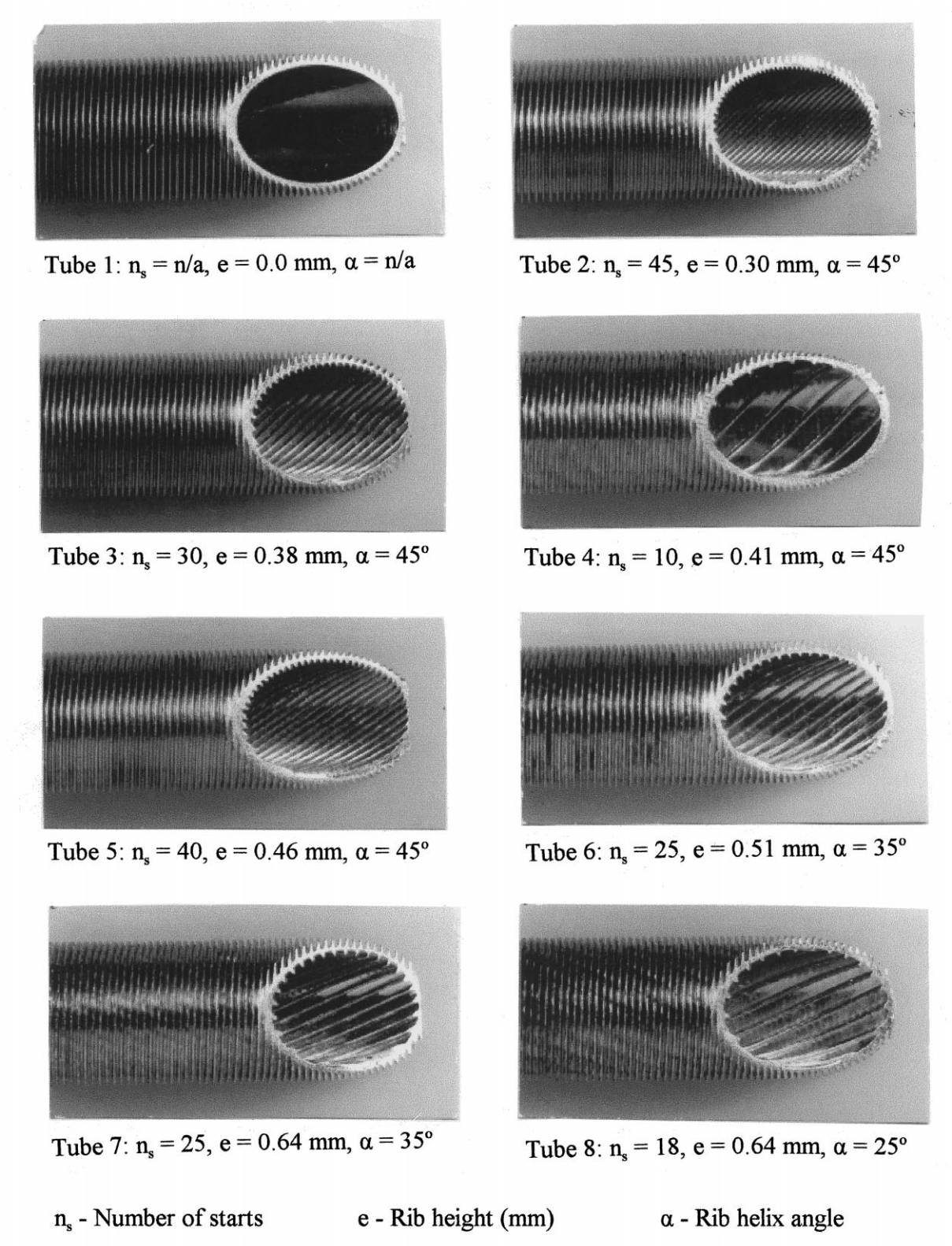

Fig. 1. Tested tube geometries.

a larger number of starts. Tubes 2, 3, and 5 are similar to enhanced tubes used today. These tubes have 25–45 starts. The greater number of starts used in Tubes 2, 3, and 5 provide higher heat transfer coefficients for water flow than the 10-start Tube 4.

If tube-side fouling occurs, the fouling will act to reduce the effective water side heat transfer coefficient (h_{eff}). The effective water side heat transfer coefficient is given by

$$\frac{1}{h_{\text{eff}}} = \frac{1}{h} + R_{\text{f}} \tag{1}$$

where h is the unfouled heat transfer coefficient, and R_{f} is the fouling resistance. In this work, the heat transfer coefficient and the fouling resistance are defined in terms of the nominal (plain tube) internal surface area ($A_{i,\text{ nom}} = \pi D_i L$). Use of the nominal area allows direct comparison of h_{i} and R_{f} with that of a plain tube.

Smooth tube refrigeration condensers are designed to accommodate $R_{\text{f}} = 4.4\text{E}-5$ m^2 K/W (0.00025 h ft^2 F/Btu) between cleaning cycles. Eq. (1) shows that the h_{eff} will be more severely reduced as the clean tube h-value increases. For example, at 1.33 m/s water velocity, the heat transfer coefficient in a plain tube will be approximately 6730 W/m^2 K. For $R_{\text{f}} = 4.4\text{E}-5$ m^2 K/W, the h_{eff} value will be 5200 W/m^2 K. Several of the tubes tested in this work provide a clean tube h-value approximately 2.3 times that of a plain tube, which is 15,480 W/m^2 K. Using $h = 15{,}480$ W/m^2 K in Eq. (1), with $R_{\text{f}} = 4.4\text{E}-5$ m^2 K/W yields 9207 W/m^2 K. Hence, for the same R_{f} a 2.3 times internal enhancement would yield only 1.77 times (9207/5200) larger h_{eff}. Hence, with $R_{\text{f}} = 4.4\text{E}-5$ m^2 K/W (0.00025 h ft^2 F/Btu) the effective enhancement factor of the enhanced tube would be reduced from 2.3 to 1.77. If the enhanced tube suffered greater fouling than a plain tube, the effective enhancement level would be further reduced. Thus, fouling control is a critical issue for such tubes.

Table 1
Tube geometry and clean tube performance ($D_{\text{i}} = 15.54$ mm, $D_{\text{o}} = 19.05$ mm, $T_{\text{b}} = 32$°C, $Re = 27{,}000$, $h_{\text{p}} = 6730$ W/m^2 K, $f_{\text{p}} = 0.0257$)

Tube	e (mm)	n_{s}	α (°)	p/e	A/A_{p}	C_{ST}	h/h_{p}	η
1	n/a	0.0	n/a	n/a	1.0	0.0277	1.0	1.0
2	0.33	45	45	2.81	1.59	0.0644	2.32	1.18
3	0.40	30	45	3.50	1.48	0.0646	2.33	1.05
4	0.43	10	45	9.88	1.17	0.0482	1.74	0.95
5	0.47	40	35	3.31	1.65	0.0628	2.26	1.04
6	0.49	25	35	5.02	1.43	0.0577	2.08	1.01
7	0.53	25	25	7.05	1.42	0.0535	1.93	1.05
8	0.55	18	25	9.77	1.31	0.0431	1.51	0.98

The clean tube performance of the Fig. 1 tubes was measured and reported by Webb et al. [9]. The Wilson plot procedure was used to obtain the water-side heat transfer coefficient, which defined the Sieder–Tate coefficient, C_{ST} used in the following equation

$$\frac{h_i D_i}{k} = C_{\text{ST}} Re^{0.8} Pr^{1/3} (\mu/\mu_w)^{0.14} \tag{2}$$

The heat transfer coefficient (h_i) is based on the nominal inside surface area defined by $A_{i,\text{ nom}}/L = \pi D_i$, where $D_i = 15.54$ mm (0.612 in.) for all tubes. The measured C_{ST} ranged from 0.02775 for the plain tube to 0.06457 for Tube 3. The C_{ST} values are listed in Table 1.

Table 1 lists the enhancement ratio (h/h_{p}) and the "effeciency index" [$\eta = (h/h_{\text{p}})/(f/f_{\text{p}})$] both calculated at $Re = 27{,}000$ using the curve fit equations. Table 1 also shows A/A_{p}, the total inside surface area, relative to that of a plain tube having $D_i = 15.54$ mm. Tubes 2, 3 and 5 show the highest h/h_{p} values and also have the greatest number of starts.

4. Fouling test apparatus and procedure

4.1. Test apparatus

Fig. 2 shows a cross-sectional view of the fouling

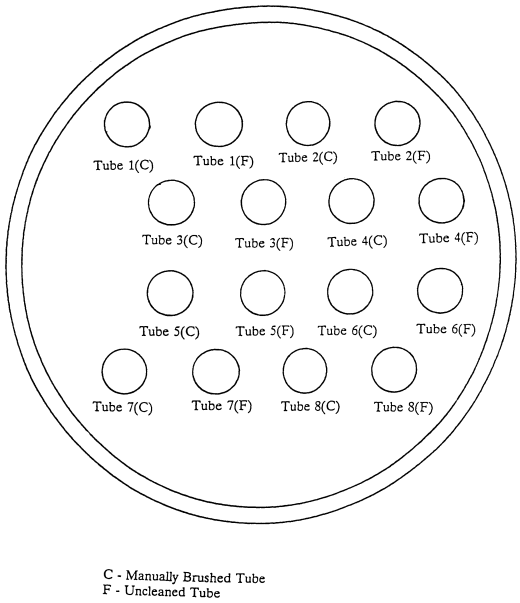

Fig. 2. Layout of paired tubes in test condenser.

test condenser. It contains 16 3.66 m (12.0 ft) long tubes, installed as eight pairs of identical tubes. Seven of the paired enhanced tubes are shown in Fig. 1, and the eighth pair is of the plain tube geometry. Reasoning for the pairs is to have one of the paired tubes run as an unfouled control and let the other tube experience long-term fouling. The unfouled condition was maintained through regular manual brushing. The tubes were horizontally paired to minimize local differences in condensing coefficient. All tubes have an identical exterior enhancement of 1023 fins/mm (26 fins/in.). The cooling tower water is circulated through the condenser in a one-pass arrangement.

Refrigerant vapor from the centrifugal compressor enters the top of the fouling condenser at two locations along the condenser length. This vapor condenses on the tubes and is drained through a manifold that empties into a sump. The condensed refrigerant is then sent back to the evaporator of the main system by a liquid-level controlled pump. The test condenser was connected to the automatic purge system of the main condenser to prevent non-condensible gas accumulation.

The present tests were conducted at the following operating conditions:

1. Water velocity of 1.07 m/s (3.5 ft/s), which yielded $Re = 16{,}000$.
2. System water having approximately 800 ppm total calcium hardness, 1600–1800 μΩ electrical resistance, and 8.5 pH.

All 16 tubes were operated at the same water velocity (1.07 m/s) throughout the test period. This velocity was set and checked using the measured pressure drop over the tube length. The friction factors of each tube were measured and reported by Webb et al. [9]. This relationship was used to set the required Δp for each tube to maintain 1.07 m/s (3.5 ft/s). The pressure drop across the tube was measured with pressure taps and a mercury U-tube manometer. A valving tree was employed, which allowed the pressure drop in each tube to be measured. A typical pressure drop for 1.07 m/s (3.5 ft/s) flow was 64 mmHg.

Water inlet and outlet temperatures were measured with thermistors in thermowells located in the fluid stream. The thermistors were installed in individual voltage divider circuits and read through a computer controlled data acquisition system. The saturation temperature of the condensing refrigerant was determined by a gauge pressure manometer and a barometer.

We had hoped to perform this test using totally untreated hard water, which would promote both biological and precipitation fouling. However, the Penn State Physical Plant was reluctant to perform the test without a biocide in the system, because this could establish a potential for Legionella. Because biological water treatment chemicals were used, no biological fouling should have been present. Hence, the test series investigated precipitation fouling (with combined particulate fouling).

The make-up water had approximately 200 ppm total calcium hardness, which resulted in operation at 4.0 concentration cycles. The water quality was monitored weekly, and analyzed by Dexter Water Services. Table 2 shows the results of a water sample analysis, which is typical of that existing during the test period. The Penn State Physical Plant maintained the water at 800 ppm (±20%) calcium hardness by checking the conductivity of the water weekly. In the other part of this work, water quality samples were taken at 26 commercial installations in the US and Canada. Analysis of these water samples showed that the system water ranged from 21 to 1044 ppm total hardness as $CaCO_3$, with a mean value of 475 ppm. The 800 ppm total hardness water used in the present tests is of significantly lower water quality than was found in the 26 city water quality survey.

The 1.07 m/s water velocity used in the present tests compares to typically used water velocities of 1.5–2.2 m/s. The lower water velocity and lower water quality were used to enhance the fouling rate, allowing the collection of meaningful results in a reasonable time period. Hence, one should note that the operating conditions used in the present tests are more severe than experienced in typical commercial systems.

4.2. Experimental procedure

Data were collected in the following manner: the unfouled control tubes were manually brushed and the condenser run for another 15 min to reach steady state after this disturbance. Eight simultaneous inlet and outlet water temperatures were measured at 10-s intervals with the computer data acquisition system. The eight simultaneous readings allow for a time averaged

Table 2
Cooling tower water sample analysis results

Parameter	Value
Hardness, total as $CaCO_3$ mg/l	705
Hardness, calcium as $CaCO_3$ mg/l	186
Hardness magnesium as $CaCO_3$ mg/l	519
Chloride, as C1 mg/l	145
Silica as SiO_2 mg/l	43
Sulfate as SO_4 mg/l	85
Alkalinity, "M" as $CaCO_3$ mg/l	509
Conductivity, micromhos at 25°C	1476
Nitrates as NO_3 mg/l	75
Phosphate, ortho as PO_4 mg/l	1

value to be obtained. During this time, an average p_{sat} was measured.

During warm weather, the data were taken on a daily basis. However, during cool weather, the load imposed on the refrigeration unit was not high enough either to provide a water temperature rise (ΔT) or to measure accurately. A water $\Delta T = 1.1^{\circ}C$, or greater, was desired for best accuracy. Small water ΔT and unsteady condensing conditions cause a high degree of scatter and poor reproducibility of the collected data.

At the start of the season, all 16 tubes (eight geometry pairs) of the test condenser were manually brushed and had an acidic solution recirculated, to dissolve any $CaCO_3$ deposits (basic) not removed by the brushing. This brought each tube to the same cleanliness start-up condition. After this, the flow rate through each of the tubes was checked by monitoring pressure drop and found to be 1.07 m/s. The system ran continuously, except for a 2-day shut at 1460 h. The test was terminated after 2500 operating hours, because of the small water ΔT late in the season.

Kim [14], Chamra [15], and Li [16] have compared the measured flow rate vs. pressure drop characteristic in the clean and fouled conditions. They found that the effect of fouling on pressure drop is very small, if the fouling resistance is less than $2.0E-4$ m^2 K/W. This is because the fouling layer is very thin. The pressure drop in each pair of tubes remained within 2% during the entire test period. Hence, we conclude that the velocity in the fouled tube was no more 2% greater than in the unfouled tube for the entire test period.

4.3. Calculation of fouling resistance (R_f)

At the start of the test, both tubes are clean, but there is a small difference (ΔR_i) between the $1/U$ values of the two tubes (ΔR_i) at start-up. The ΔR_i is calculated as the difference between the $1/U$ values of the two tubes at the start-up (initial) condition.

$$\Delta R_i = \frac{1}{U_{f,\,i}} - \frac{1}{U_{c,\,i}} \tag{3}$$

where $1/U_f$ refers to the tube that is allowed to foul, and $1/U_c$ refers to the tube that is manually cleaned. The subscript "i" indicates the start-up condition. After fouling has initiated, the fouling resistance is calculated by difference between the two paired tubes. This is given by

$$R_f = \frac{1}{U_f} - \left(\frac{1}{U_c} + \Delta R_i\right) \tag{4}$$

Note that $1/U$ and R_f (m^2 K/W) are based on the plain tube internal surface area taken at the base of the fins. By defining the surface area in terms of the nominal tube diameter (15.54 mm), the R_f values of all tubes may be directly compared.

The UA value was determined by the following equation:

$$\frac{1}{UA} = \frac{\Delta T_{lm}}{q} \tag{5}$$

4.4. Error analysis

An error analysis, using the method of Kline and McClintock [10], was performed. The errors introduced by the initial measurement of flow rate versus pressure drop were assumed to be negligible when compared to the absolute pressure drop reading to establish the desired flow rate. A fairly strong indirect dependence was found with chiller load. In the induction period (<1350 h), under high chiller load conditions (4.4°C water temperature rise), the error is $\pm 5.67E-6$ m^2 K/W. Under light load (1.38°C water temperature rise), the error increases to $\pm 1.1E-5$ m^2 K/W. Typically, the water ΔT was between 2.2 and 3.8°C. The experimental uncertainty in R_f was $\pm 1.1E-5$ m^2 K/W during the 1350 h induction period. This uncertainty is 25% of the manufacturer's condenser design, rating fouling resistance of $\pm 4.4E-5$ m^2 K/W (± 0.00025 h ft^2 F/Btu).

A repeatability test in a subsequent year revealed that the beginning fouling values show a range of $1.07E-7$ to $1.92E-5$ m^2 K/W standard deviation units, ignoring one tube, which had a value of $1.04E-4$ m^2 K/W standard deviation units. All of the collected points for this test fell within $\pm 3\sigma$.

5. Fouling test results

Fig. 3a–h show the measured fouling resistance for each of the eight tube geometries listed in Table 1. These figures show that no significant fouling occurred in any of the tubes for approximately 1350 operating hours. After this time, all eight tubes started to show some fouling. However, significant fouling increase was observed for Tubes 2, 3, and 5, with the greatest increase occurring in Tube 2. Tubes 1 (plain tube) and 4 (10 starts) showed the smallest R_f increase. Tubes 6, 7 and 8 showed a moderately small R_f by the end of the cooling season.

The asymptotic fouling resistance R_f^* is controlled by the water hardness, concentration of airborne dust in the water, the water velocity, the tube wall temperature, and the internal surface geometry. To limit our discussion of the fouling mechanism, we will focus on the fouling resistance values listed in

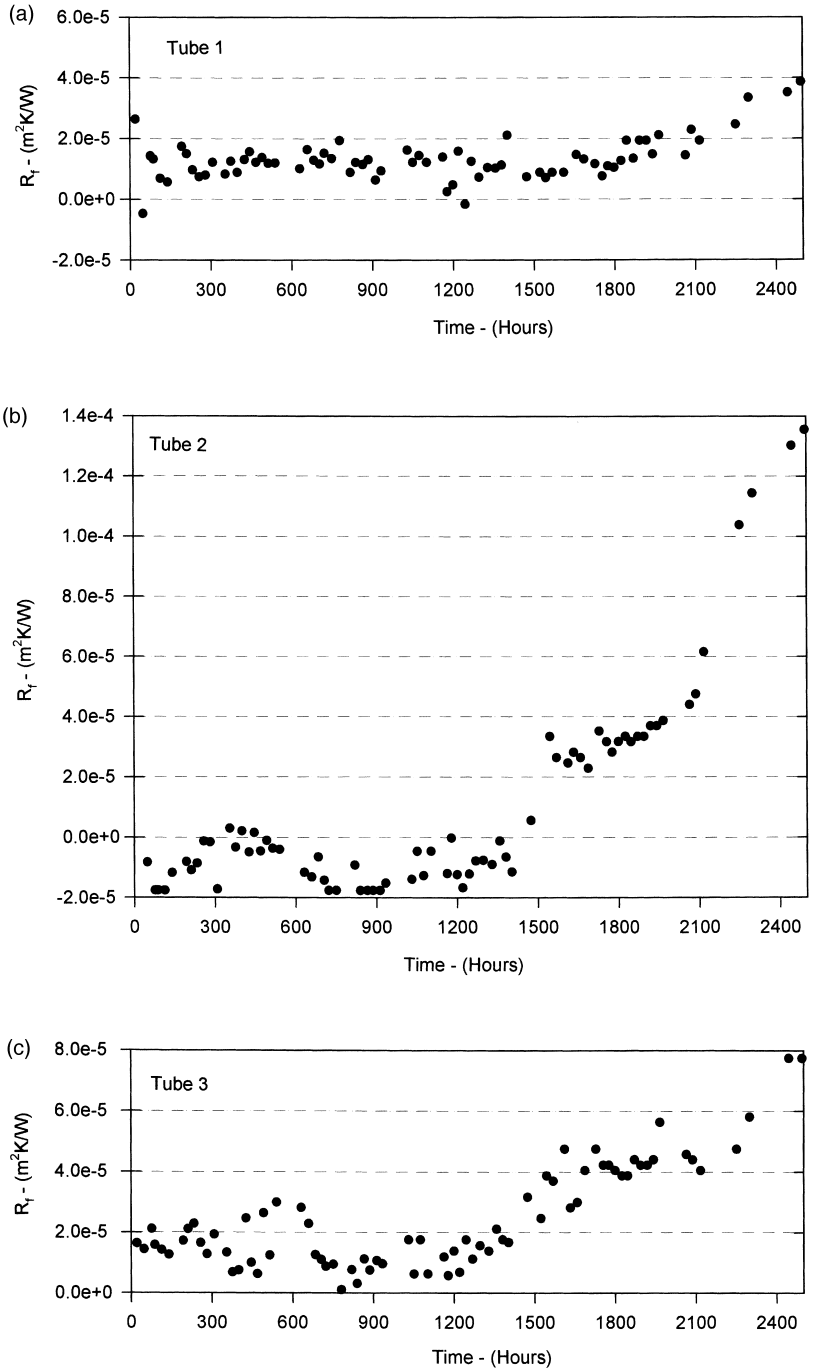

Fig. 3. Fouling data for the Fig. 1 tubes: (a) Tube 1, (b) Tube 2, (c) Tube 3, (d) Tube 4, (e) Tube 5, (f) Tube 6, (g) Tube 7, (h) Tube 8.

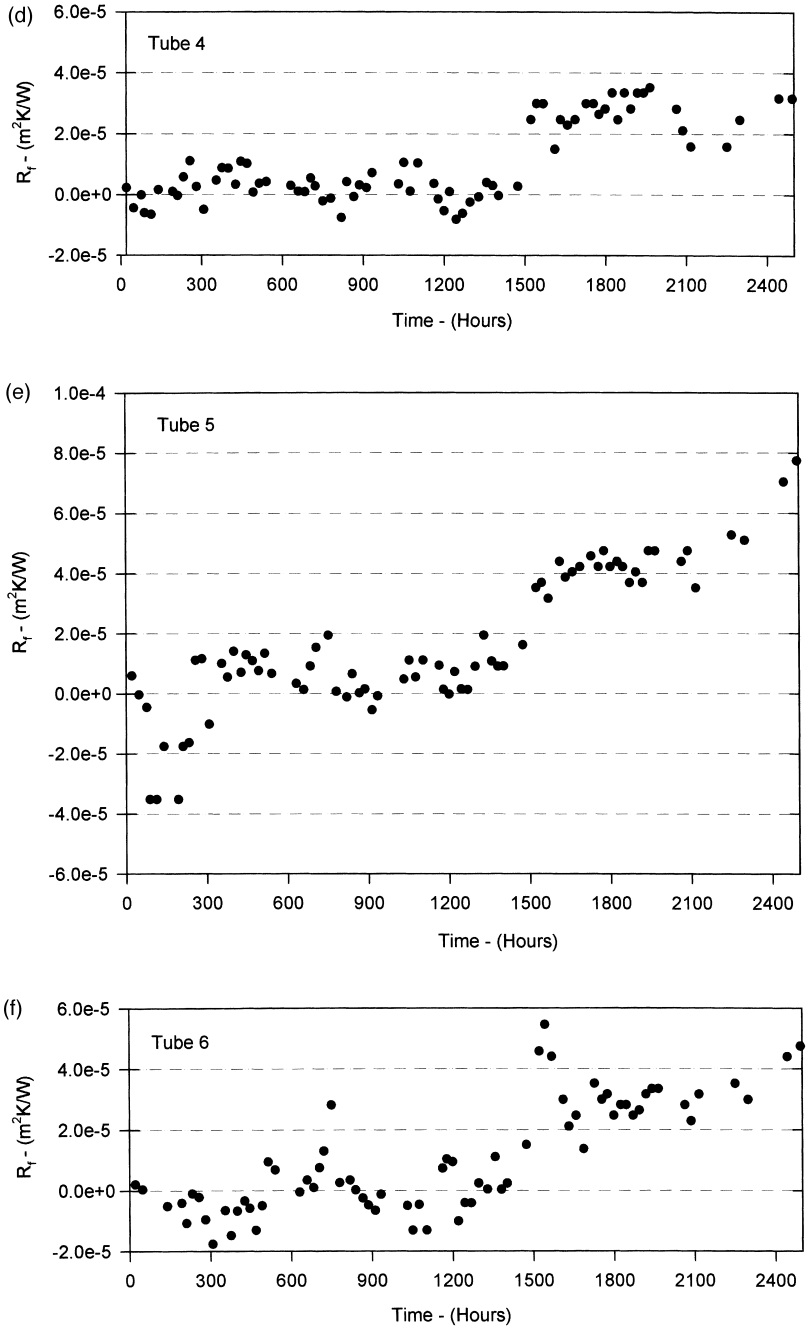

Fig. 3 (*continued*)

Table 3. The table lists the final fouling resistance (R_f) at the end of the season (column 2) along with the tube geometry specifications. The tubes are listed in order of decreasing R_f values. Table 3 shows that Tubes 2, 3, and 5 had experienced very significant fouling by the end of the cooling season. For Tube 2, the measured R_f is 3.25 times the design value, as compared to the plain tube having only 64% of the design R_f. Tube 4, which has the smallest number of internal fins, has the smallest R_f value compared to the other internally enhanced geometries.

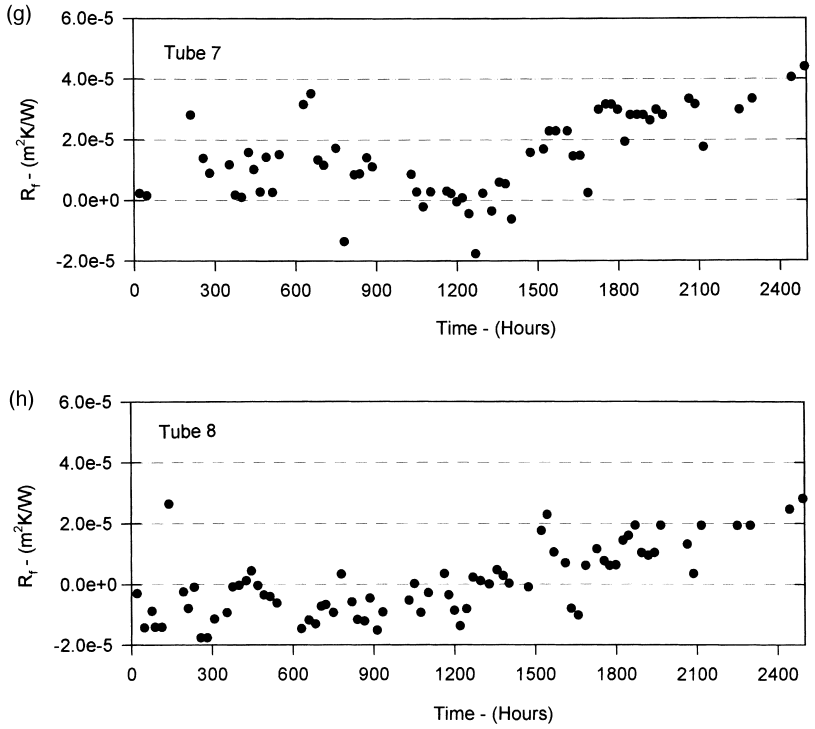

Fig. 3 (*continued*)

Fig. 4 shows photographs of several of the fouled tubes that were removed from the fouling condenser after the tests were completed. Fig. 4 shows that significant physical deposits exist in the interfin region of Tubes 2 and 5, with the greatest amount appearing in Tube 2. The deposits were of a soft and "fluffy" nature and could be removed by brushing with a Nylon bristle brush. The powder removed from fouling deposit has the same appearance and structure as the particulate fouling deposit in Li and Webb [13]. Chemical analysis of the fouling deposits is presented and discussed in Li and Webb [13], which shows that 40% of the fouling deposits do not contain calcium. If the deposits were caused only by precipitation fouling they would be a hard scale and have high calcium content.

5.1. Repeatability of the experimental data

A repeat test series sought to reproduce the fouling that was measured in a following cooling season. The cooling tower water system was being operated at six cycles of concentration (e.g., 1200 ppm hardness as

Table 3
Fouling resistance vs. tube geometry (at the end of 2500 h test period)

Tube	$R_f \times 10^4$ (m^2 K/W)	$R_f \times 10^4$ (repeat test) m^2 K/W	n_s	e (mm)	α (°)	p/e	h/h_p
2	1.44	1.71	45	0.33	45	2.81	2.32
5	0.95	1.0	40	0.47	35	3.31	2.26
3	0.63	0.92	30	0.40	45	3.50	2.33
6	0.44	0.46	25	0.49	35	5.02	2.08
7	0.42	0.42	25	0.53	25	7.05	1.93
8	0.35	n/a	18	0.55	25	9.77	1.51
4	0.32	0.49	10	0.43	45	9.88	1.74
1	0.28	0.40	n/a	n/a	n/a	n/a	1.0

$CaCO_3$) as compared to 800 ppm. The tube side velocity in each tube was held at 1.19 m/s (3.9 ft/s). The results are shown in column 3 of Table 3. Because the hardness of repeat test season is larger than that of original cooling season, it is reasonable that the fouling resistance of each tube in column 3 should be larger than that of each tube in column 2. The fouling rates are generally repeatable.

6. Discussion of fouling data

6.1. Induction period

Precipitation fouling has an induction period, during which nucleation sites are established. Then the fouling deposits begin to accumulate. The present fouling mechanism is one of combined precipitation and par-

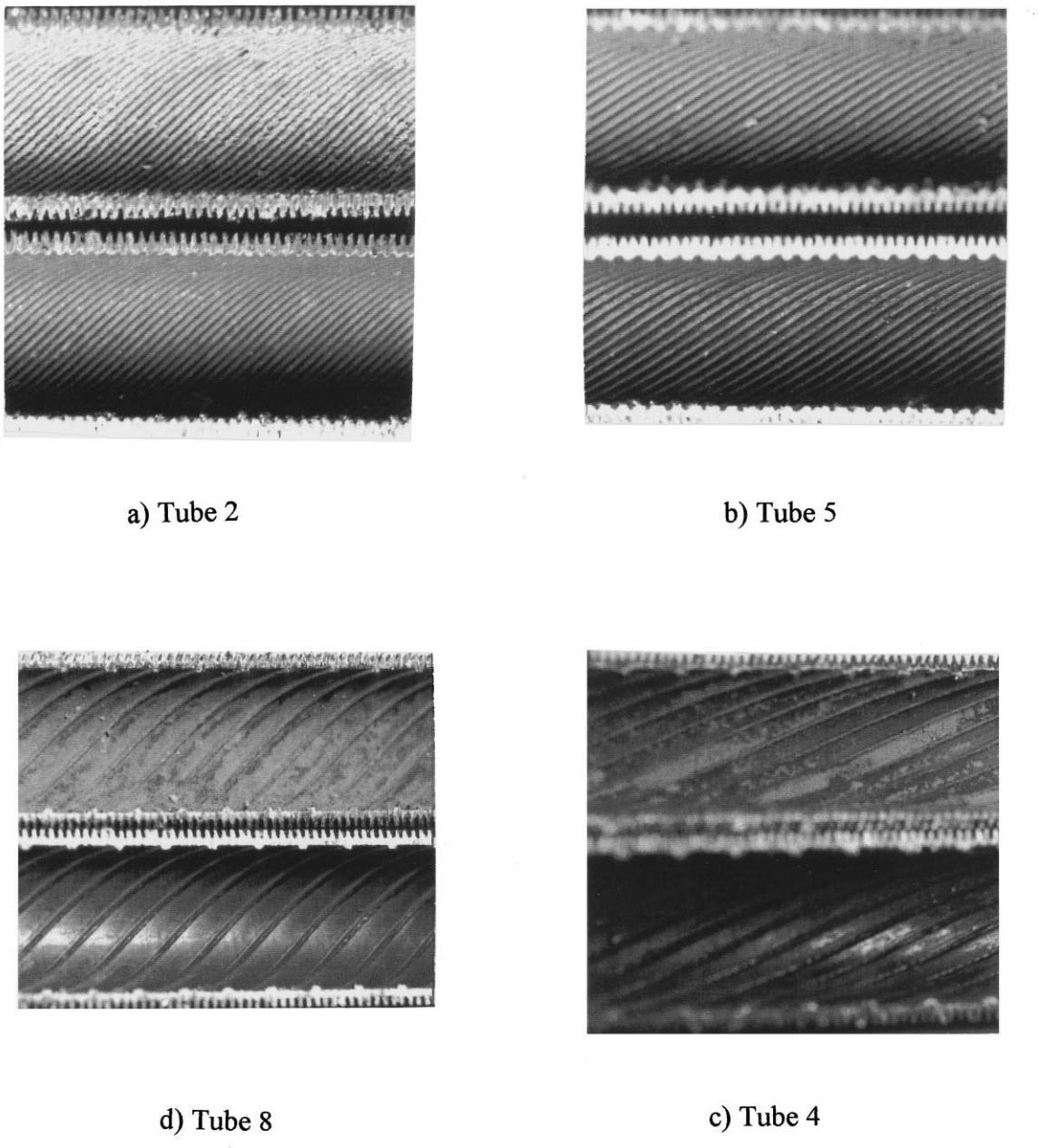

Fig. 4. Photos of fouled (upper photo) and unfouled (lower photo) tubes after completion of tests.

ticulate fouling. Time is needed for fouling conditions to be established. During this induction period, nucleation sites are slowly established with the involvement of suspended particles in the water. The data indicate that the induction period (θ_D) is approximately 1350 operating hours for the presently tested tubes. Both the enhanced tube and plain tube have almost the same induction period. After the induction period, the fouling conditions are established, and the fouling resistance begins to increase. Beginning at approximately 1350 operating hours, we began to see fouling in all the tubes.

For all types of fouling, Hasson [11] proposed that the delay time decreases with an increase in surface roughness. He argued that surface indentations provide regions amenable to deposition because they are sheltered from the bulk velocity. Additionally, the surface roughness increases the contact surface area such that the true contact area is much larger than the apparent surface area. However, our data show that the induction periods are the same for smooth surface and the "rough" surfaces tested.

The apparent effects of precipitation fouling are shown by the delay time in the fouling curve. No delay time was shown in particulate fouling as reported by Kim and Webb [1], Somerscales et al. [2] and Chamra and Webb [3]. Bansal et al. [12] investigated the effect of crystallizing and non-crystallizing particles on crystallization fouling of calcium sulphate in a plate heat exchanger. Fig. 6 of their paper clearly shows the effect of filtration on precipitation fouling. Under the same conditions, fouling data without filtration show no roughness delay; fouling data with a 20 μm filter show a short roughness delay; and fouling data with 1 μm filter show a longer roughness delay. Because no filtration was used in the present system, it is not surprising that both particulate and precipitation fouling existed.

6.2. Effect of pitch and height ratio

Fig. 5 shows the relation between fouling resistance and the number of internal fin starts. Fig. 5 shows that R_f is strongly influenced by the number of starts. The greatest fouling increase occurred in Tubes 2, 3, and 5, which have 45, 30, and 40-starts, respectively. Tubes 5 and 6 both have 35 degree helix angle. However, the 40 start Tube 5 shows significantly higher R_f than does the 25 start Tube 6. As the number of starts is increased, the axial pitch between ridges decreases and provides sheltered, low velocity areas for the initial growth of the fouling deposit. The decreased shear stress in the interfin region should support the initial development of the fouling deposit, and result in a lower removal rate of the deposited material. Further discussion of the envisioned fouling mechanism is given in Part II of the paper of Li and Webb [13].

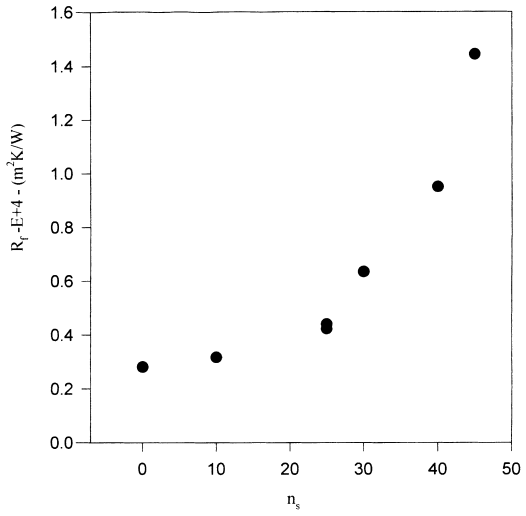

Fig. 5. Relation between fouling resistance and number of starts.

7. Implications of study

This study has shown that use of tubes having a large number of starts and helix angles in range of 40° can result in significant fouling after a long time period, if operated at high $CaCO_3$ hardness and low water velocity. However, the test conditions used here are more severe (higher hardness and lower water velocity) than are used in typical commercial systems. These test results cannot be used to infer what fouling results will exist for higher water velocity or lower hardness. More data are required for such operating conditions.

The salient finding of this work is that the potential for fouling increases as the number of starts and helix angle increases. Should fouling be found for such tubes, one may avoid significant fouling penalty by following good maintenance practices. This means keeping the water treated and operation at a moderate number of concentration cycles. Tube cleaning at the end of the cooling season, or use of on-line cleaning systems are viable options.

8. Conclusions

Fouling data were obtained for a 2500 h operating period using system water of approximately 800 ppm hardness. The water was treated to prevent only biological fouling. The water used was in the 90th percen-

tile of the water qualities found in 26 installations across the US.

Based on observed fouling deposits, the mechanism of fouling is combined precipitation and particulate fouling. The induction period was 1350 h, after which an increase of fouling was observed in all tubes. The greatest fouling increases occurred in Tubes 2, 3, and 5; these tubes experienced significant fouling by the end of the cooling season. These three tubes have the greatest number of starts and helix angles between 35 and 45°. The greatest fouling occurred in Tube 2, which had 45 starts. The final R_f was 3.25 times the design value of $R_f = 4.4E-5$ m^2 K/W (0.00025 h ft^2 F/Btu).

Because of the high hardness and low water velocity used in these tests, we do not believe that the fouling experienced is typical of that expected in commercial installations. With use of good maintenance practices and water quality control, all the tubes tested are probably suitable for long-term fouling applications.

Acknowledgements

This project was principally funded by EPRI, with additional financial support from The Trane Co., Carrier Corp., and Wolverine Tube Corp. Mr. Wayne Krill served as EPRI Program Manager. Program Coordinators representing the industrial participants were Mr. Lou Mougin (Trane), Dr. Robert Chiang (Carrier), and Mr. Petur Thors (Wolverine). Wolverine made all the special test section tubes used in this work. Mr. Jerry Tripp, of The Trane Co., and Mr. Julian DeBullet, of Carrier Corp. directed the field water quality sampling program. Ms. Amanda Meitz at Dexter Water Services provided support for the water chemical analysis. At Penn State, two Research Assistants served principal roles. Mr. Larry Scherer was instrumental in the design and construction of the fouling apparatus. Then, Mr. Wei Li assumed responsibility for the test program. We are very appreciative of the support provided by all of these program participants and sponsors.

References

[1] N.-H. Kim, R.L. Webb, Particulate fouling of water in tubes having a two-dimensional roughness geometry, Int. J. Heat Mass Transfer 34 (11) (1991) 2727.

[2] E.F.C. Somerscales, A.F. Ponteduro, A.E. Bergles, Particulate fouling of heat transfer tubes enhanced on their inner surface, Fouling and Enhancement Interactions HTD-Vol. 164 (1991) 17.

[3] L.M. Chamra, R.L. Webb, Modeling liquid-side particulate fouling in enhanced tubes, Int. J. Heat Mass Transfer 37 (4) (1994) 571.

[4] A.P. Watkinson, Fouling of augmented heat transfer tubes, Heat Transfer Engineering 11 (3) (1990) 57.

[5] R.W. Morse, J.G. Knudsen, Effect of alkalinity on the scaling of simulated cooling tower water, Canadian Journal of Chemical Engineering 55 (1977) 272.

[6] R.L. Webb, Principles of Enhanced Heat Transfer, Wiley/Interscience, New York, 1994 (Chapter 10).

[7] T.J. Rabas, et al., Comparison of power-plant condenser cooling-water fouling rates for spirally-indented and plain tubes, Fouling and Enhancement Interactions HTD-Vol. 164 (1991) 29.

[8] S.I. Haider, R.L. Webb, An experimental study of tube-side fouling resistance in flooded water chiller evaporators, ASHRAE Transactions 98 (Part 2) (1992) 86–103.

[9] R.L. Webb, R. Narayanamurthy, P. Thors, Heat transfer and function characteristics of internal helical-rib roughness heat transfer and friction, J. Heat Transfer 122 (2000) 122–134.

[10] S.J. Kline, F.A. McClintock, Describing uncertainties in single-sample experiments, Mechanical Engineering 75 (1953) 3–8.

[11] D. Hasson, Progress in precipitation fouling research — a review, in: Proceedings of Fouling Mitigation of Industrial Heat-Exchange Equipment, An International Conference, Begell House, 1997.

[12] B. Bansal, H. Muller-Steinhagen, X.D. Chen, Effect of suspended particles on crystallization fouling in plate heat exchangers, J. Heat Transfer 119 (1997) 568–574.

[13] W. Li, R.L. Webb, Fouling in enhanced tubes using cooling tower water Part II: combined particulate and precipitation fouling, Int. J. Heat and Mass Transfer 43 (2000) 3579–3588.

[14] N.-H. Kim, Fouling in enhanced tubes having arc-shaped two-dimensional roughness geometry, Ph.D. Thesis, The Penn State University, 1989.

[15] L.M. Chamra, A theoretical and experimental study of particulate fouling in enhanced tubes, Ph.D. Thesis, The Penn State University, 1992.

[16] Wei Li, A theoretical and experimental study of fouling in enhanced tubes in cooling tower systems, Ph.D. Thesis, The Penn State University, 1998.